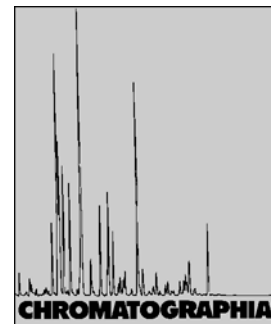


# Development of Rigid Biporous Polymeric Adsorbent for Protein Chromatography



2002, 55, 405–410

Y. Shi / X.-Y. Dong / Y. Sun\*

Department of Biochemical Engineering, School of Chemical Engineering and Technology, Tianjin University, Tianjin 300072, P.R. China;  
E-Mail: ysun@tju.edu.cn

## Key Words

Column liquid chromatography  
Biporous matrix  
In situ co-polymerization  
Proteins

## Summary

A novel biporous poly (glycidyl methacrylate-triallyl isocyanurate-divinylbenzene) resin (denoted as Resin C) was prepared by *in-situ* co-polymerization with both superfine granules of sodium sulfate and the solvents toluene and n-heptane as porogenic agents. This material is based on a novel porogenic mode of a combination of both solid granules and solvents. The properties of Resin C were characterized, and then compared with both Resin A (where only solvents as porogen) and Resin B (where only solid granules are used as porogen). The biporous resin showed good mechanical performance, high dynamic adsorption capacity and column efficiency at high flow-rates. These factors indicate the biporous resin as a promising adsorbent for high-speed protein separation by chromatography.

## Introduction

Liquid chromatography is an important and powerful technique in the separation and purification of biomolecules, especially proteins [1, 2]. The stationary phase for chromatography is the key element in the development of this technology. Great advances have occurred related to the design and production of high performance liquid chromatographic media since diethylaminoethyl derivatized cellulose was first used for the separation of proteins by Sober and Peterson [3]. Continuous research work is being made to find better stationary phases to satisfy the

needs of high performance protein separation and purification [4].

When designing a chromatographic medium it is necessary to meet a compromise between high capacity, rapid kinetics, and mechanical strength [5]. Conventional rigid porous supports rely on high surface area, and hence high binding capacity, provided by an internal pore structure of pore size on the order of 10 to 100 nm [6]. However, mass transfer of solute molecules occurs through such stationary phase beads by diffusion. Diffusion is as a slow process, especially in the case of proteins that present high molecular mass and low diffusion coefficient [4].

In order to circumvent this obstacle, small non-porous beads (1–4  $\mu\text{m}$ ) had been proposed as an alternative. These small beads do not have “stagnant mobile phase mass transfer and mass transfer is no longer a problem [7]. Therefore, much faster separation can be easily achieved [8, 9]. However, these beads are of limited application in protein separation and purification because of their low binding capacities and low column permeability. Therefore, perfusion chromatography was developed in the early 1990s. This technology employs convective mass transfer into the bead interior by creating matrices that contain large channels (>600 nm) connected to smaller diffusion pores (30–70 nm) [1]. Perfusive beads combine the high binding capacity of conventional porous supports, with improved mass transfer character of non-porous bead. This combination gives great advantages to this type of stationary phase in protein separation and purification [4]. However, it is notable that the preparation of perfusive beads involves a very complicated process, including preparing small particles using suspension, emulsion, or hybrid polymerization techniques and then building up particles into matrices of 5–10  $\mu\text{m}$  [10]. Recently, the concept of a novel porogenic way, the cooperation of solid granule and solvent, was developed in our laboratory [11]. This achievement provides a new approach to produce high-performance biporous chromatographic media with a simple procedure, although the drawback of low mechanical stability of the biporous matrix needed to be overcome.

In a previous publication, a novel macroporous poly(glycidyl methacrylate-triallyl isocyanurate-divinylbenzene) anion-exchanger has been successfully prepared for protein adsorption in our laboratory [12]. In this present work, a rigid biporous chromatographic media with the same polymer skeleton and superfine granules of sodium sulfate, toluene and n-heptane as porogenic agents was prepared by *in-situ* co-polymerization. The use of toluene and n-heptane, instead of cyclohexanol and lauryl alcohol adopted by Zhang and Sun [11], as porogenic agents was intended to enhance the mechanical performance of the medium based on our previous research [12]. After anion-exchange groups were introduced by epoxy opening reaction with diethylamine, the matrix (denoted as Resin C) was used as an anion-exchanger. The properties of Resin C were characterized and compared with those of Resin A (with only solvents as porogen) and Resin B (with only solid granules as porogen).

## Experimental

### Materials

Glycidyl methacrylate (GMA) (99%) was purchased from Suzhou Anli Chemical Corp. (Jiangsu, China) and used without further purification. Triallyl isocyanurate (TAIC) was kindly donated by Professor X. Q. Guo, Nankai University (Tianjin, China). Divinylbenzene (DVB) (45% divinyl monomer) was purchased from Shanghai Qunli Chemical Factory (Shanghai, China) this was extracted with 10% aqueous sodium hydroxide and distilled water, dried over anhydrous magnesium sulfate, and then distilled under vacuum. Toluene and n-heptane were products of Tianjin Chemical Corp. (Tianjin, China). 2,2'-Azobis(isobutyronitrile) (AIBN) was obtained from Tianjin Dagu Chemical Factory (Tianjin, China) and was recrystallized in ethanol before use. Sodium sulfate was purchased from Tianjin Yifa Chemical Factory (Tianjin, China). Superfine granules of sodium sulfate crystalline was prepared by addition of hot ethanol (50 °C) to saturated sodium sulfate solution at 50 °C. The particle size distribution was measured with a Mastersizer 2000 particle size analyzer (Malvern Instrument Ltd., UK). The result indicated that the particle sizes of 90% sodium sulfate crystallines were between 0.7–1.5 μm. All pro-

teins reported in this study were purchased from Sigma (St Louis, MO, USA). Other reagents were all of analytical grade and used as received.

### Synthesis of Solid Matrices

In general, the porogenic agents – solvents (toluene and n-heptane, 1.5:1 *mollmol*) and/or granules of sodium sulfate were added to a mixture of monomers (GMA, DVB and TAIC, 1:0.17:0.17 *mollmol mol*), in which the free radical initiator, AIBN (2 mol % with respect to monomers) was dissolved. Various compositions of the polymerization mixtures for preparing Resins A, B and C were 100/67/0, 100/0/40 and 100/67/40 (monomers/solvent/solid granule, *v/v/v*), respectively. These mixtures were degassed and well mixed in an ultrasonicator for 30 min. The mixtures were then poured into a glass tube (100 × 10 mm I.D.) which was sealed at one end. The other end of the tube was then sealed. The temperature of *in-situ* co-polymerization was linearly raised from 45 °C to 65 °C within 1 h, held at 65 °C for 3 h, then 75 °C for 1 h and finally 85 °C for 2 h. This program of temperature changes was chosen to ensure that the co-polymerization did not occur too rapidly and to avoid the bubble formation. This procedure led to the formation of a white solid rod within the tube. The whole co-polymerization reaction has been described by Yu and Sun [12]. Once the co-polymerization was completed, the polymer rod was pushed out and then ground into small particles. The solvent porogenic agents, toluene and n-heptane, were stripped by extracting the particles with ethanol under reflux for at least 24 h in a Soxhlet extraction apparatus. The solid porogenic agent, sodium sulfate, was washed from the particles with 30% ethanol solution until no precipitation in the supernatant could be detected by the addition of BaCl<sub>2</sub>. The particles were then dried under vacuum (<130 Pa) at room temperature, and fractionated by sieving with 34- and 74-μm standard test sieves.

### Preparation of Anion Exchangers

The modification of the particles for the preparation of anion exchangers is based on ring-opening reaction of the epoxide groups on the co-polymer as described elsewhere [12]. In summary 5.0 g resin was

mixed with 25 mL diethylamine and 25 mL dioxane, and the mixture was stirred and heated at 60 °C for 6.5 h. Any epoxide groups remaining on the polymer were reduced to hydroxyl groups by suspending in 100 mL of 0.1 M NaBH<sub>4</sub> solution and shaking it overnight in a shaking incubator (140 rpm) at room temperature. Finally, the product was thoroughly washed with an excess of distilled water and ethanol. This was repeated 10–15 times over a week, and finally dried at 50 °C for 24 h until constant weight.

### Characterization of the Particles

The particle size distribution was measured with Mastersizer 2000 particle size analyzer. The pore size distribution analysis was performed on a Micromeritics AUTOPORE II 9320 automated mercury porosimeter by mercury intrusion porosimetry. Scanning electron microscopy (SEM) was carried out on a XL30 ESEM scanning microscope (Phillips, Netherlands) to characterize the pore structures of the particles in dry state. All samples were sputter-coated with gold before analysis. The specific surface areas of the dry particles were determined by the three-point nitrogen adsorption (BET) method, with a BET ST-03 instrument. The water contents of the resins were determined according to Wu and Brown [13].

### Static Adsorption Isotherms

The standard batch adsorption system was utilized to determine the static adsorption isotherms of the anion exchangers for using bovine serum albumin (BSA) as a model protein [14]. Typically, 0.05 g wet resin was introduced into a test tube containing 5 mL BSA solution. The initial BSA concentrations were from 0.2 to 2.0 mg · mL<sup>-1</sup>. Adsorption was performed at 25 °C in a shaking incubator (120 rpm) for 24 h. At the end of adsorption, solid phase was centrifugally separated and the supernatant was analyzed at 280 nm for residual protein concentration. The equilibrium protein concentration and the amount of protein adsorbed onto the anion exchangers were calculated by mass balance.

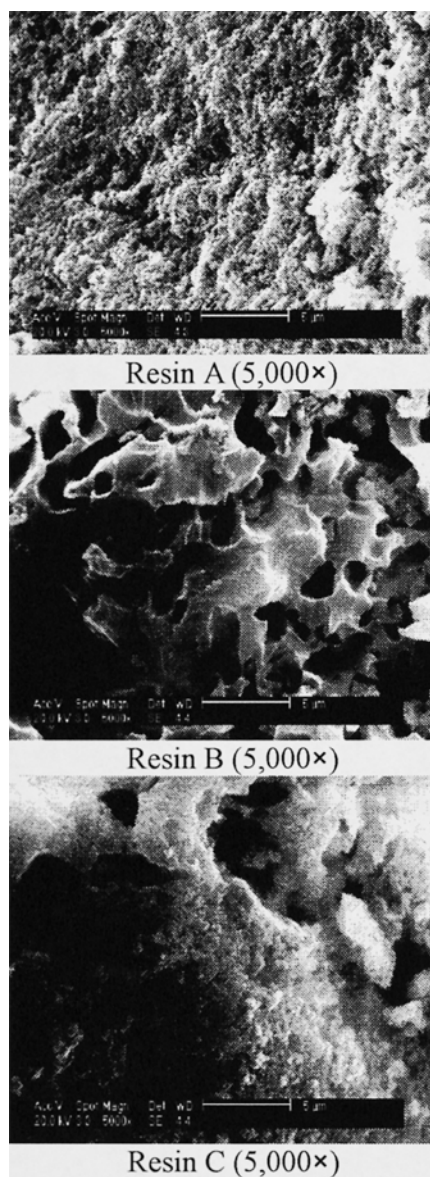


Figure 1. Scanning electron micrographs of the matrices.

## Chromatography

The volume-weighted mean diameters of Resins A, B and C were 60.5, 54.3 and 54.1  $\mu\text{m}$ , respectively. These particles were packed into chromatographic columns ( $30 \times 4.6$  mm I.D., 0.5 mL volume) to produce Columns A (with Resins A), B (with Resin B) and C (with Resin C). An ethanol slurry packing technique was used for the column packing. All packed-bed chromatography experiments were carried out using a Waters HPLC system consisting of a controller, a 600E pump, a manual injector with an injector loop of 5  $\mu\text{L}$  (Rheodyne 7725i, Australia) and a 2478 UV detector. PC 800 software (Waters, Milford, MA, USA.) was used for data acquisition and processing was used. The flow beha-

avior of the columns was determined by measuring the back-pressure as a function of mobile phase flow velocity with 0.01 M Tris-HCl buffer pH 7.6 (buffer A) as the mobile phase.

The dynamic adsorption capacity was determined by frontal analysis. The column was equilibrated with 10–15 column volumes (CVs) of buffer A. After taking the column off-line, the tubing before the column was purged with 30 mL of  $2 \text{ mg} \cdot \text{mL}^{-1}$  BSA solution. The column was then brought on-line and loaded with feed until the absorbance of the outlet stream has approached that of the inlet stream. Then, the column was eluted with 30 CVs of 1 M NaCl, and re-equilibrated. Based on the UV signals, the level of breakthrough was determined by normalizing the protein concentration with the initial protein concentration. The dynamic capacity was calculated by

$$q_{10} = \frac{cF(t_{10} - t_0)}{V_B} \quad (1)$$

$$q_{50} = \frac{cF(t_{50} - t_0)}{V_B} \quad (2)$$

where  $q_{10}$  and  $q_{50}$  are the dynamic capacities at 10 and 50% breakthrough, respectively,  $c$  is the feed BSA solution concentration,  $t_{10}$  and  $t_{50}$  are the time of 10 and 50% breakthrough, respectively,  $t_0$  is the retention time under non-retained condition,  $F$  is volumetric flow-rate and  $V_B$  is the bed volume (0.5 mL).

The column efficiencies were measured by elution chromatography. Lysozyme and BSA were used as the detectors. In these experiments, a 5- $\mu\text{L}$  pulse of protein solution was injected into the column and the eluted peak was recorded at the column exit. The dead volume of the system was measured by injecting 5  $\mu\text{L}$  of 50% acetone solution via the injection loop. The experiments were conducted at flow-rates ranging from 72 to 1260  $\text{cm} \cdot \text{h}^{-1}$ .

The column efficiency was expressed as the height equivalent to a theoretical plate ( $H$ ), which was determined from the following equation:

$$H = \frac{\sigma^2 L}{\mu_1^2} \quad (3)$$

where  $L$  is the column length (30 mm),  $\sigma^2$  is the peak variance and  $\mu_1$  is the first moment (mean). From the experimental chromatogram,  $\mu_1$  and  $\sigma^2$  are calculated from

$$\mu_1 = \frac{\int_0^\infty tc(t)dt}{\int_0^\infty c(t)dt} \quad (4)$$

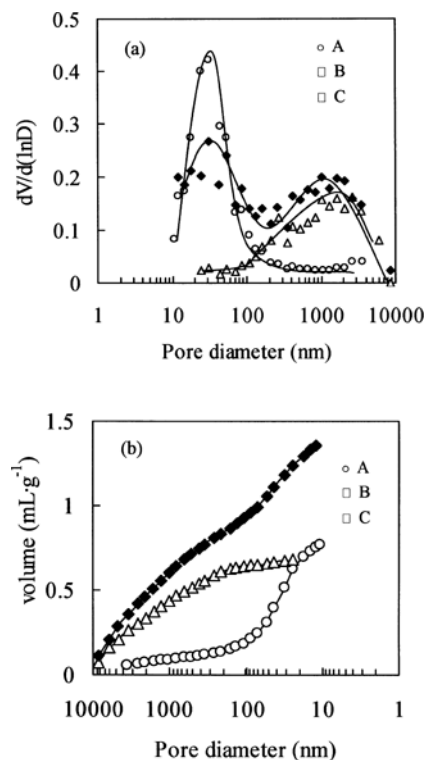


Figure 2. Pore size distributions of the matrices. (a) Incremental intrusion distribution; (b) Cumulative intrusion distribution.

and

$$\sigma^2 = \frac{\int_0^\infty t^2 c(t)dt}{\int_0^\infty c(t)dt} - \mu_1^2$$

where  $t$  is time and  $c(t)$  is elution concentration of protein at the column exit.

## Results and Discussion

### Characteristics of the Matrices

The variance in pore structures of Resins A, B and C is evident from the SEM photographs (Figure 1). It can be seen that Resin A has a so-called “spongy” appearance [5], which is suggestive of wide, open micropores. Resin B is composed of a continuous three-dimensional polymer phase and irregular macropores formed by the presence of the solid granules. Resin C when compared with Resins A and B, shows regions of micropores similar to Resin A and of macropores similar to Resin B. More detailed pore size analysis is shown in Figure 2. Here, the data is plotted as  $dV/d(\log D)$  (Figure 2a) and the cumulative intrusion volume (Figure 2b) against pore diameter, where  $V$  is the volume of mercury which has penetrated and  $D$  is the pore diameter. Obviously, Resin A, with solvent as the porogenic agent, and Resin

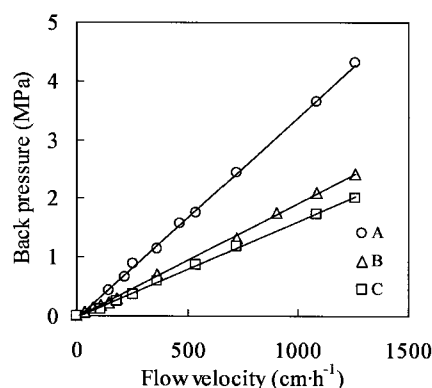


**Figure 3.** Effect of liquid flow-rate on back-pressure of a column packed with 37–74  $\mu\text{m}$  beads. Conditions: column  $30 \times 4.6$  mm I.D.; mobile phase 0.01 M Tris-HCl buffer pH 7.6.

B, with solid granules as the porogen, both contain one family of pores in the range of about 10–150 and 150–3000 nm with a distinct maximum near 30 and 1500 nm, respectively. In contrast, for Resin C, with both the solvents and the solid granules as the porogen, a typical bimodal distribution is identified clearly (Figure 2a). The large-size pores correspond to flow-through pores (200–3000 nm) that serves as the intraparticle flow channels, and the small-size pores to a population of small diffusive pores (10–150 nm) that contribute more significantly to the specific area. The difference between these three pore size distributions can be explained in terms of the roles of different porogenic agents. The solvent porogenic agents are the main contributors to the regions of the micropores, while the solid granules contribute to the regions of the macropores. Thus, similar to the conventional porous media with solvents as porogen, the size of micropores and macropores in Resin C can be designed by adjusting the composition of the polymerization mixture [15] and the size of solid granules, respectively. Here, the pore structure of Resin C appears to be more suitable for convective mass transfer in contrast to that of our previously prepared biporous resin [11].

When the separation medium is used for chromatography, a high binding capacity is essential. The specific surface area is one of the main indicators of its binding capacity. The specific surface areas of Resins A, B and C are 44.0, 4.0 and  $35.2 \text{ m}^2 \cdot \text{g}^{-1}$ , respectively when determined by the BET method. The somewhat smaller specific surface area of Resin C, compared to Resin A, is due to the presence of macropores [16].

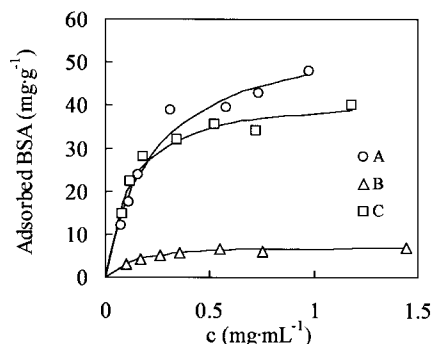


**Figure 4.** Static adsorption isotherms of BSA to the anion-exchange resins.

Water contents of Resins A, B and C are estimated at 57.1, 64.1 and 67.7 ( $w/w$ )%, respectively. It is notable that the polymer skeleton, procedure of preparation, and crosslinking degree of the three resins are the same, therefore the most likely explanation of the relatively high water content of Resin C is the existence of macropore structure.

### Flow Behavior of Packed Columns

For a resin to be used in a HPLC, it should be rigid and stable when its packed column is operated at elevated flow-rates. Figure 3 shows the effect of flow-rate on back-pressure in a packed column. A linear dependency of the back-pressure on the mobile phase flow-rate is observed up to a superficial linear velocity of  $1260 \text{ cm} \cdot \text{h}^{-1}$ . This reveals that little compression or damage of the particles occurred under the operation conditions. In our previous work [11], the biporous chromatography medium could only be operated below  $720 \text{ cm} \cdot \text{h}^{-1}$ ; and at flow rate higher than  $1000 \text{ cm} \cdot \text{h}^{-1}$ , the back-pressure increased drastically due to breakage of the irregular-shape resin. Compared with that, the mechanical strength of the biporous resin developed here is greatly improved. This is due to the use of toluene and n-heptane as the porogens instead of cyclohexanol and lauryl alcohol [11]. It can also be seen that at this highest flow-rate tested, the back-pressures of Columns B and C are lower than that of Column A.

### Adsorption Capacity

The static BSA adsorption isotherms of the three resins are presented in Figure 4.

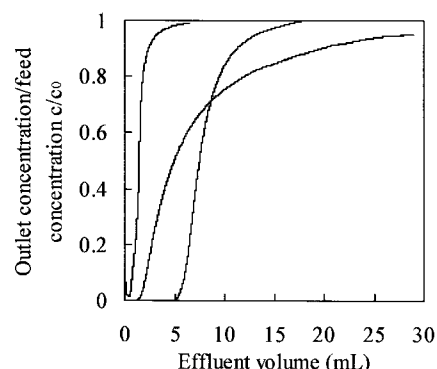


**Figure 5.** Breakthrough curves for BSA at  $180 \text{ cm} \cdot \text{h}^{-1}$ . Conditions: column  $30 \times 4.6$  mm I.D.; mobile phase 0.01 M Tris-HCl buffer pH 7.6; feed BSA concentration  $2 \text{ mg} \cdot \text{mL}^{-1}$ ; UV detection at 280 nm.

The solid lines are calculated from the Langmuir equation:

$$q = \frac{q_m c}{K_d + c} \quad (6)$$

where  $q$  ( $\text{mg} \cdot \text{g}^{-1}$  wet resin) is the adsorbed BSA density to the adsorbent,  $q_m$  is the adsorption capacity,  $c$  ( $\text{mg} \cdot \text{mL}^{-1}$ ) is the equilibrium concentration of BSA in bulk solution, and  $K_d$  ( $\text{mg} \cdot \text{mL}^{-1}$ ) is the dissociation constant.  $q_m$  and  $K_d$  are determined by fitting the equilibrium data to the Langmuir equation with the non-linear Simplex method. The static BSA capacities of Resins A, B and C are estimated are 55.3, 7.4 and  $42.8 \text{ mg} \cdot \text{g}^{-1}$  wet resin, respectively. These correspond well with the specific surface areas of the resins described above. Using the data of the wet density of the Resin C ( $1.08 \text{ g} \cdot \text{mL}^{-1}$ ) and assuming a packed-bed voidage of 0.35 [17], it is estimated that the capacity of Resin C is  $30.1 \text{ mg} \cdot \text{mL}^{-1}$  bed column. This value is higher than some commercially available biporous anion-exchange media for the same model protein [18].

One of the most important characteristics of a chromatography column is its dynamic adsorption capacity. Differences in the static and dynamic binding capacities of an adsorbent is a sensitive measure of mass transfer limitations [19, 20]. Frontal analysis provides the dynamic adsorption data. Figure 5 illustrates BSA breakthrough curves at  $180 \text{ cm} \cdot \text{h}^{-1}$  for Columns A, B and C. The 10% breakthrough adsorption capacity of Columns A and B are 8.8 and  $4.5 \text{ mg} \cdot \text{mL}^{-1}$  bed column (or 12.5 and  $6.4 \text{ mg} \cdot \text{g}^{-1}$  wet resin), respectively, while for Column C a capacity of  $24.4 \text{ mg} \cdot \text{mL}^{-1}$  bed column (or  $34.8 \text{ mg} \cdot \text{g}^{-1}$  wet resin =  $37.5 \text{ mg} \cdot \text{mL}^{-1}$ ) is ob-

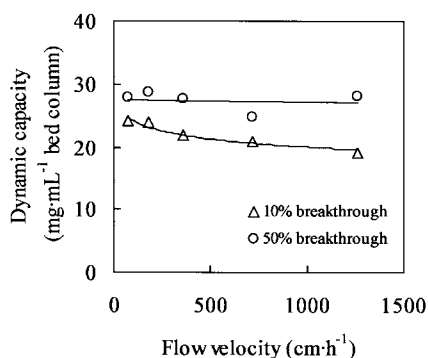


**Figure 6.** Dynamic capacity of BSA on Column C at 10 and 50% breakthroughs as a function of flow-rate.

tained. The dynamic capacity of Column A decreased considerably when compared with the static capacity determined by batch experiments that allow saturation of binding sites. This is due to the intrinsically low intra-particle diffusive mass transfer in Resin A. The dynamic capacities of Resins B and C, on the other hand, are close to their static capacities respectively. These prove that in the case of Resin C, BSA molecule permeates the particles by a combination of convective and diffusive mass transport due to the presence of the flow-through macropores, and thus the rate of mass transfer is accelerated.

In order to further confirm the conclusion that the intra-particle mass transfer in Resin C is greatly enhanced by convection, the dynamic adsorption capacities of Resin C were measured at elevated flow-rates. The capacities at 10 and 50% breakthrough as a function of flow-rate are shown in Figure 6. The results indicate that the dynamic capacity at 10% breakthrough decreases less than 20% when the flow-rate increases up to  $1260 \text{ cm} \cdot \text{h}^{-1}$ , while the capacity at 50% breakthrough is approximately unchanged.

It has been reported that the dynamic capacities (10% breakthrough) of commercially available polymer-based anion-exchange resins, i.e., POROS QE/M, Macro-Prep 25Q, Fractogel EMD TMAE 650s and Source 30Q at a flow-rate range of  $144$  to  $720 \text{ cm} \cdot \text{h}^{-1}$  for BSA are 38, 21, 28 and  $38 \text{ mg} \cdot \text{mL}^{-1}$ , respectively [21]. Obviously, the dynamic capacity of Resin C is higher than that of Macro-Prep 25Q and Fractogel EMD TMAE 650s, and comparable to that of POROS QE/M, the typical commercial biporous anion-exchange resin, and Source 30Q.

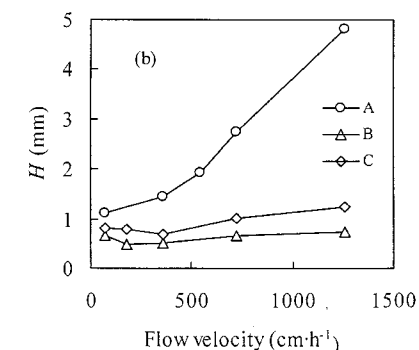
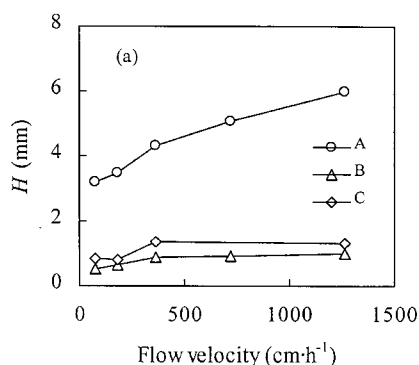


**Figure 7.** Column efficiency detected with (a) lysozyme and (b) BSA as a function of mobile flow-rate. Conditions: column  $30 \times 4.6 \text{ mm}$  I.D.; injection volume  $5 \mu\text{L}$ ; UV detection at  $280 \text{ nm}$ . (a) mobile phase  $0.01 \text{ M}$  Tris-HCl buffer  $\text{pH}$  7.6; feed lysozyme concentration  $5 \text{ mg} \cdot \text{mL}^{-1}$ ; (b) mobile phase  $0.2 \text{ M}$  NaCl in  $0.01 \text{ M}$  Tris-HCl buffer  $\text{pH}$  7.6; feed BSA concentration  $10 \text{ mg} \cdot \text{mL}^{-1}$ .

### Column Efficiency

The chromatographic efficiency of the resins as a function of flow-rate is represented in Figure 7a (lysozyme) and Figure 7b (BSA). Lysozyme was non-retained because it is positively charged [22], while BSA was weakly retained under the experimental condition. It can be seen that Columns B and C are of much greater efficiency than Column A. Moreover, the  $H$  values of Columns B and C are approximately unchanged in the range of mobile phase velocities for both the proteins, while that of Column A increases significantly with the flow-rate.

The elution chromatograms of both proteins obtained at  $360 \text{ cm} \cdot \text{h}^{-1}$  are shown in Figure 8a (lysozyme) and Figure 8b (BSA). It is clear that the tailing of the elution peak for Column A is much more significant than those of Columns B and C. Extra-column contributions to band-broadening are negligible since the injection size and the volume of the extra-column tubing and fittings are much smaller than the width of the observed peaks. There-

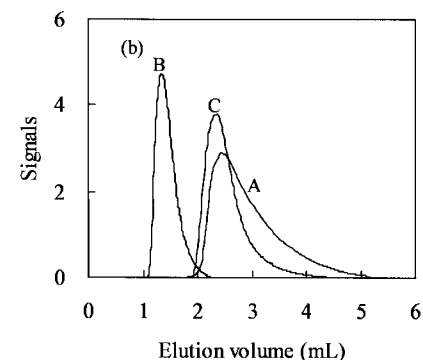
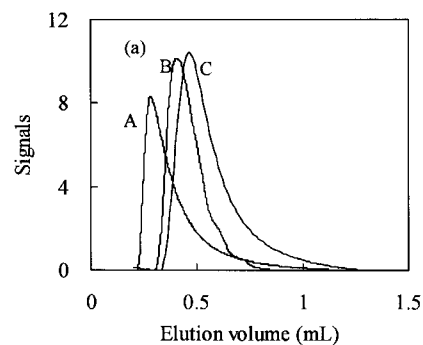


**Figure 8.** Chromatograms of (a) lysozyme and (b) BSA. Experiments were performed at  $360 \text{ cm} \cdot \text{h}^{-1}$ . Other conditions were the same as in Figure 7.

fore, these can be well explained in terms of the pore structures of the resins. Mass transfer in Resin A is a diffusion-limited case, so there is higher diffusive resistance in Resin A and its column efficiency decreases with increasing the mobile phase flow-rate [23]. Conversely, accelerated mass transfer resulting from the presence of flow-through pores in Resin C (a diffusion-convection case) substantially reduces the negative effect of micropore diffusion on the plate height. Therefore column efficiency is nearly the same with that of Resin B with only macropores (Figure 7) and the tailing of elution peak for Column C is not so significant as Column A. The macropores allow the mass transport of protein molecules into the interior part of the particle by convective flow, leading to high column efficiency at elevated flow-rates [2, 24].

It has been reported that the column plate heights for lysozyme of columns packed with  $21.8 \mu\text{m}$  POROS 20SP and  $26.6 \mu\text{m}$  SP POROS 20 OH beads at non-retained conditions was  $0.87$  and  $1.20 \text{ mm}$  respectively at  $1222 \text{ cm} \cdot \text{h}^{-1}$  [16]. The re-

sults presented here indicate that the column efficiency of Resin C is comparable to those of the commercially available biporous polymeric media that have smaller particle size.

## Conclusions

An ideal medium for protein separation is biporous materials with high specific surface area, large pores required for high capacity, low flow resistance and good mechanical strength. We have developed a novel porogenic mode, i.e., and combination of solid granules and solvents, which simplifies the preparation of biporous media into a simple in situ co-polymerization. A biporous co-polymer of GMA, DVB and TAIC was produced using granules of sodium sulfate and toluene and n-heptane as porogenic agents, and was then employed as an anion exchanger after functionalized with diethylamine. Results from SEM and mercury intrusion porosimetry measurements reveal that the matrix contains regions of micropores with a maximum at approximately 30 nm and regions of macropores with a distinct maximum near 1500 nm. In contrast to the resins using only solvents or solid granules as porogenic agent, the biporous medium simultaneously possessed a high specific surface area of  $35.2 \text{ m}^2 \cdot \text{g}^{-1}$  and a high water content of 67.7%. The column packed with this biporous medium showed a low back-pressure at mobile phase flow velocity up to  $1260 \text{ cm} \cdot \text{h}^{-1}$ , indicating its good mechanical perfor-

mance. Because of the presence of flow-through pores, the dynamic adsorption capacity was as high as  $34.8 \text{ mg} \cdot \text{g}^{-1}$  wet resin, close to its static capacity. In addition, the column packed with this material exhibited high column efficiency as detected with lysozyme and BSA as model proteins. These results highlight that the flow-through pores in the biporous resin substantially increase the mass transfer rate of the large molecules and minimize the negative effects of diffusion. Thus, it is considered that the biporous resin is a promising adsorbent for high-speed protein separation.

## Acknowledgement

This research was supported by the National Natural Science Foundation of P. R. China (grant No. 20025617).

## References

- [1] Afeyan, N.B.; Gordon, N.F.; Mazsaroff, I.; Varady, L.; Fulton, S.P.; Yang, Y.B.; Regnier, F.E. *J. Chromatogr. A* **1990**, *519*, 1–29.
- [2] Afeyan, N.B.; Fulton, S.P.; Regnier, F.E. *J. Chromatogr. A* **1991**, *544*, 267–279.
- [3] Sober, H.A.; Peterson, E.A. *J. Am. Chem. Soc.* **1954**, *76*, 1711–1712.
- [4] Garcia, M.C.; Marina, M.L.; Torre, M. *J. Chromatogr. A* **2000**, *880*, 169–187.
- [5] Hunter, A.K.; Carta, G. *J. Chromatogr. A* **2000**, *897*, 65–80.
- [6] Whitney, D.; McCoy, M.; Gordon, N.; Afeyan, N.B. *J. Chromatogr. A* **1998**, *807*, 165–184.
- [7] Chase, H.A. *J. Chromatogr. A* **1984**, *297*, 179–202.
- [8] Colwell, I.F.; Hartwick, R.A. *J. Liq. Chromatogr.* **1987**, *10*, 2721–2744.
- [9] Lee, D.P. *J. Chromatogr. A* **1988**, *443*, 143–153.
- [10] Afeyan, N.B.; Regnier, F.E.; Dean, R.C. *U.S. Pat.* **1991**, 5,019,270.
- [11] Zhang, M.L.; Sun Y. *J. Chromatogr. A* **2001**, *922*, 77–86.
- [12] Yu, Y.H.; Sun, Y. *J. Chromatogr. A* **1999**, *855*, 129–136.
- [13] Wu, G.; Brown, G.R. *Reactive Polymers* **1991**, *14*, 49–61.
- [14] He, L.Z.; Gan, Y.R.; Sun, Y. *Bioprocess Eng.* **1997**, *17*(5), 301–305.
- [15] Guyot, A.; Bartholin, M. *Prog. Polym. Sci.* **1982**, *8*, 277–331.
- [16] Nash, D.C.; Chase, H.A. *J. Chromatogr. A* **1998**, *807*, 185–207.
- [17] Brown, G.G. *Unit Operations*, Wiley, New York, **1950**.
- [18] Levison, P.R.; Mumford, C.; Streater, M.; Brandt-Nielsen, A.; Pathirana, N.D.; Badger, S.E. *J. Chromatogr. A* **1997**, *760*, 151–158.
- [19] Van Deemter, J.J.; Zuiderweg, F.J.; Klintonberg, A. *Chem. Eng. Sci.* **1956**, *5*, 271–289.
- [20] Deen, W.M. *AIChE J.* **1987**, *33*, 1409–1425.
- [21] Staby, A.; Jensen, I.H.; Mollerup, I. *J. Chromatogr. A* **2000**, *897*, 99–111.
- [22] Kegbubgerm, A.L. *Principles of Biochemistry*, Worth Publishers, New York, **1982**.
- [23] Rendueles de la Vega, M.; Chenou, C.; Loureiro, J.M.; Rodrigues, A.E. *Biochem. Eng. J.* **1998**, *1*, 11–23.
- [24] Liapis, I.; McCoy, M.A. *J. Chromatogr. A* **1992**, *599*, 87–104.

Received: Sep 10, 2001  
Revised manuscript  
received: Dec 10, 2001  
Accepted: Jan 2, 2002